NASA Technical Memorandum 106980

In-Orbit Calibration of a SAMS Triaxial Sensor Head

Louis S. Chestney
Aerospace Design & Fabrication, Inc.
Brook Park, Ohio

and

Ronald J. Sicker
Lewis Research Center
Cleveland, Ohio

June 1996

National Aeronautics and
Space Administration

IN-ORBIT CALIBRATION OF A SAMS TRIAXIAL SENSOR HEAD

Louis S. Chestney
Aerospace Design & Fabrication, Inc.
Brook Park, Ohio 44142

and

Ronald J. Sicker
National Aeronautics and Space Administration
Lewis Research Center
Cleveland, Ohio 44135

SUMMARY

This report describes the results of in-orbit calibration data collected for a Space Acceleration Measurement System (SAMS) Triaxial Sensor Head (TSH) and the methods used to process the data for bias and gravity levels.

INTRODUCTION

Space Acceleration Measurement System (SAMS) Triaxial Sensor Heads (TSH's) are designed to measure low-level vibrations in a microgravity (μg) environment. Each TSH is composed of three identical circuit paths containing a Sundstrand QA-2000 accelerometer connected to a 1-pole combination low-pass filter and preamplifier, followed by a 7-pole low-pass filter then an analog to digital converter (ADC). Each sensor outputs a signal that is of the form M = G + B, where M is the magnitude of the data measured and recorded by the system, G is the magnitude of the input acceleration, and B is the magnitude of the bias of the sensor head electronics (particularly the accelerometer bias). This equation can be manipulated in units of counts, volts, or μg's. Since actual measurements are recorded in counts, an implicit conversion factor from counts to volts C_v, and a second conversion factor from volts to μg (S) is necessary. For purposes of this report μg will be used in calculating the values of this equation.

The value of M is the quantity measured in space while the values of S and B are derived from a fourth order equation as a function of temperature. C_v is the conversion factor of 10 V/65536 counts. The coefficients used in the equations for bias and scale factor are obtained from measurements obtained during a calibration procedure performed on Earth. Several errors arise during this process (ref. 1). Many of these errors arise because it is being done in the 1-g environment of Earth while the SAMS TSH has been designed to operate in a μg environment. The procedure described in the following section was designed for the dual role of improving the current SAMS measurement by reducing bias error and also characterizing the accuracy of measurements that may be obtained by using a similar automated procedure in the SAMS–II, the follow-on advanced SAMS unit.

METHOD

During the Space Shuttle mission STS–60, SAMS unit A flew in the Spacehab–2 middeck augmentation module. The SAMS calibration procedure was performed on a 5-Hz TSH at MET 005/11:12 (DDD/HH:MM) to 005/11:30, and again at MET 006/00:56 to 006/01:06 as part of SAMS nominal operations. The operation performed at MET 005/11:12 to 005/11:30 was scheduled preflight, and was performed during a "semi-quiet" time, while the operation performed at MET 006/00:56 to 006/01:06 was an in-flight adaption done while other operations were going on, particularly movement of the Canadian robot arm. A quiet time is required to ensure that all accelerations are symmetrical to avoid introducing a positive or negative bias in the data.

The SAMS calibration procedure consisted of rotating the SAMS TSH π radians in the YZ-plane and collecting data for a few minutes. A second set of data was obtained when the TSH was rotated back to its original orientation. Rotation of the TSH in the YZ-plane provides data for Y- and Z-axis calibrations while maintaining X-axis data as a control.

The mathematical rational for this procedure is as follows. With the TSH oriented at 0 radians, measurement M_0 is described as

$$M_0 = G_0 + B_0 \tag{1}$$

where G_0 is the constant acceleration, and B_0 is the DC bias of the system at 0 radians. With the TSH oriented at π radians, measurement M_π is described as

$$M_\pi = G_\pi + B_1 \tag{2}$$

where G_π is the constant acceleration and B_1 is the DC bias of the system at π radians. If the time duration between data sets M_0 and M_π is kept sufficiently small, then bias B_0 equals bias B_1. Furthermore, acceleration G_0 equals negative G_π. Thus, equation (2) becomes

$$M_\pi = -G_0 + B_0 \tag{3}$$

Algebraic manipulation yields the following:

$$G_0 = (M_0 - M_\pi)/2 \tag{4}$$

$$B = (M_0 + M_\pi)/2 \tag{5}$$

APPLICATION

Processing of the SAMS data was performed for the time slices containing each of the TSH orientations. Processing consisted of first sorting the raw data into sequential samples for each axis. The data sequence was then converted into units of gravity (G) using the ground-based calibration model for scale factor, calculated at the temperatures measured in flight during each facet of the procedure.

The data collected at MET 005/11:12 to 005/11:30 were used to analyze data at the transition when the TSH was rotated back to its initial position,[1] while the data collected at MET 006/00:56 to 006/01:06 were used to analyze data at the transitions when the TSH was rotated to its new position as well as back to its initial position.

Figure 1 shows acceleration data collected between MET 006/00:47 and MET 006/01:07 for the shuttle Y-axis. The vertical axis is in units of microgravity (μg), which is 10^{-6} Earth gravity units, while the horizontal axis is in units of seconds from the start of the data file being shown. The large spikes in the center and right of the graph were caused by the rotation of the sensor head during the calibration procedure. The first of these two spikes occurred when the TSH was rotated π radians from the normal position (shown between points B and C), while the second spike occurred when the TSH was rotated back to its normal position of 0 radians (shown between points F and G). The spike at time B-C corresponds to the time period labeled as time 2 while the spike at time F-G corresponds to the time period labeled as time 3 in the tables in this report. The spike at the left of the graph is a disturbance prior to the beginning of the procedure that has no effect on the procedure.

These data were converted from units of SAMS counts into units of G by multiplying each sample by its ideal scale factor. The ideal scale factors were computed for each axis and time period as a function of the average temperature and amplification level during the measurement period. These amplification levels were 100, 100, and 10 for the X-, Y-, and Z-axes, respectively. The average temperatures are given in table 1, while the average scale factors are given in table 2. Times labeled as forward are the times when the TSH was oriented in the direction it was at during the predominant portion of the flight, while times labeled as reverse are times when the TSH was oriented in the direction rotated π radians in the YZ-plane. Analysis was performed on segments of data just before the TSH

[1] SAMS data just prior to the TSH rotation at MET 005/11:12 to 005/11:30 were not available because both of SAMS optical disks were filled prior to implementation of the calibration procedure.

was rotated (represented by data segments A-B, and E-F), and just after the TSH was rotated (represented by data segments C-D, and G-H). Selection of time segments that were close together in time was a high priority in order to ensure that the basic acceleration environment remained as constant as possible.

Figure 2 shows the time slice of data used for calculating the Y-axis semiprocessed (data converted to μg without applying the bias compensation) mean for the time segment from MET 006/00:56:24 to MET 006/00:57:24. This time period occurred just after the sensor head was rotated π radians.

Table 3 shows the mean acceleration values obtained at each of the three TSH orientation transitions. Indicated time 1 is at MET 005/11:30, time 2 is at MET 006/00:56, and time 3 is at MET 006/01:06. Table 4 shows the calculated ambient acceleration for the Y- and Z-axes of the TSH at the respective time intervals. Study of these data indicates a reasonable correspondence between the ambient acceleration measurements at each time interval for both axes. The values displayed in table 4 were calculated with equation (4). The values displayed in table 5 were calculated with equation (6).

Because the sensor was rotated in the YZ-plane, G_0 and G_π in equations (1) and (2) are equal for the X-axis. Thus, equation (6) is obtained by subtracting equation (2) from equation (1).

$$\left(M_0 - M_\pi\right) = \left[G_0 + B_0 - \left(G_0 + B_0\right)\right] = 0 \tag{6}$$

This value should thus be zero. Since we know the actual value for the X-axis measurement is zero and the measurements and calculations were performed in the same way for the X-axis as for the Y- and Z-axes, we can use the X-axis as a control for the Y- and Z-axes. Specifically, the errors associated with the X-axis measurements are typical of the bias and ambient gravity measurement error of all axes.

The errors associated with the X-axis in table 5 are not of great concern for ambient gravity measurements when the environment was noisy because the values of acceleration for both the Y- and Z-axes are an order of magnitude greater than that of the bias and ambient gravity measurement error reported for the X-axis. This may not be the case when the environment is quiet, however. These errors are never a problem with the bias measurements because the errors are always at least two orders of magnitude or less than the bias as is shown in table 6.

Table 6 shows the calculated biases (using eq. (5) and data from table 3) for the Y- and Z-axes of the TSH at the respective time intervals. The X-axis data are, however, invalid because the sensor was rotated in the YZ-plane. Because of this, G_0 and G_π in equations (1) and (2) are equal. Thus, equation (3) is invalid and equation (5) for the X-axis calculation becomes

$$B' = \left(M_0 + M_\pi\right)/2 \rightarrow \left(G_0 + B_0 + G_0 + B_0\right)/2 \rightarrow G_0 + B_0 = M_0 \tag{7}$$

This equation is only true when the acceleration $G_0 = 0$ and thus it provides no useful information to us.

A closer look at the data in table 6 shows a close correspondence for the Y- and Z-axes. Study of these data indicates a reasonable correspondence between the bias measurements at each time interval for the Y-axis, and for the Z-axis between times 2 and 3, which were close together. The difference in Z-axis bias at time 1 can be associated with many factors. Two possible factors are a general difference in environment between time 1 and the set of times 2 and 3 for a combination of Z-axis temperature and acceleration. Additional factors are a change in the environment during the procedure, making it invalid, or an actual sensor bias shift. The Z-axis temperature had an inherent uncertainty due to the way the data was collected, however, the Y-axis temperature differed by only 0.4 °C between the two data set groups. The temperature profile did show a change in the slope in the middle of the procedure however. This is illustrated in figure 3. This factor would have introduced the effect of sensor hysteresis on the calculation. This effect would also affect the ambient acceleration measurement. The method just described works well in an ideal situation but has drawbacks in the real world. Of primary concern is how to use this data to improve our acceleration data, while compensating for bias changes induced by changes in the temperature of the accelerometers.

In order to incorporate the on-orbit–bias-measurement calibration into the flight data, this procedure needs to be repeated at various temperatures. This may be impractical. An alternative approach would be to adjust the ground-based calibration data by an amount determined from the in-flight calibration method. This can be accomplished by comparing the in-flight bias calculation with the bias calculated with the ground-based calibration model at the same temperature, then shifting the ground-based bias model to fit the in-flight measured bias.

A method of checking the accuracy of the ground-based bias calculation is to apply the complete processing model, including bias compensations to the flight data, then repeat the process for determining the bias as it was performed above. The resultant bias derived from these calculations would be zero if the ground-based bias compensation model was perfect. Any difference represents the error in the ground-based bias model. Towards this goal processing of the data was done using zero offset correction,[2] as well as bias, scale factor, and axis misalignment processing.[3]

Figure 4 shows the processed acceleration data collected between MET 006/00:47 and MET 006/01:07 for the shuttle Y-axis. As with the semiprocessed data in figure 1, the large spikes in the center and right of the graph were caused by the rotation of the sensor head during the calibration procedure. As previously, analysis was performed on segments of data just before and after the TSH was rotated. Figure 5 shows the time slice of data used for calculating the processed Y-axis mean for the time segment from MET 006/00:56:35 to MET 006/00:57:15.

Table 7 shows the mean acceleration values obtained at each of the three TSH orientation transitions. Times 1 to 3 and orientations of forward and reverse are the same times and orientations used in the previous tables. The term unfiltered is used to distinguish this data from data in the next section that is low-pass filtered.

Table 8 shows the calculated ambient acceleration for each axis of the TSH at the respective time intervals. Study of this data also indicates a reasonable correspondence between the ambient acceleration measurements at each time interval for both the Y- and Z-axes. The errors associated with the X-axis in table 9 are of similar magnitude to those shown in table 5.

Table 10 shows the calculated model-bias errors for the Y- and Z-axes of the TSH at the respective time intervals. While the values of calculated model-bias error in table 10 are far smaller then the calculated absolute bias calculations in table 6, the numbers in table 10 are at least an order of magnitude larger than the bias measurement errors for the procedure shown in table 9, and are therefore not a problem. Similar to the absolute bias measurements made previously, the method just described has some drawbacks as well. Of particular concern are changes in the G environment during the calibration procedure. One disturbance of particular concern was movement of the Canadian robot arm when our calibration procedures were being performed.

By definition the bias is an approximately constant signal. Because of this, our results should be improved by filtering out the higher frequency disturbances that may cause asymmetrical accelerations. When one is filtering the data for analysis, special care must be taken to avoid transient effects caused by the response time of the filter to steplike inputs. These effects were avoided in our processing by ensuring that a sufficient number of data points had been processed through the filter before the analysis was performed.

Figure 6 shows the same data as in figure 4, after it has been filtered by a low-pass filter with a pass band of 0.01 Hz. As with the previous data, the large spikes in the center and right of the graph are caused by the rotation of the sensor head at times 2 and 3 during the calibration procedure.

Figure 7 shows the subset of data used for calculating the X-axis filtered mean. The time period shown is the same used for the unfiltered mean in figure 5.

Tables 11 to 14 show results of the same calculations in tables 7 to 10, except that the calculations were performed on data that have been low-pass filtered at a pass band of 0.01 Hz. Comparisons between the filtered and unfiltered data for ambient gravity level can best be done on the controlled TSH axis X because this actual value is known to be zero because the X-axis sensor was not rotated (refer to eq. (6)), while the value for the Y- and Z-axis values are unknown. Comparison of the X-axis values show that the average filtered magnitude is 0.3718 μg versus 0.3682 μg for unfiltered data, thus a slightly better answer is obtained from the unfiltered data. The sum of both data sets indicates that the accuracy of the data is ±0.6142 μg as determined by the largest difference from zero. A value of 0.2491 μg is more realistic, however, as will be discussed later in this report when an analytical accuracy is presented with the t-statistic used as the basis.

Comparisons between the filtered and unfiltered data for calculated model bias error can only be done on the measured TSH axes Y and Z because no information was obtained on the controlled X-axis. Comparison of the

[2]Zero offset processing involves subtracting out the bias of the SAMS electronics. Zero offset data is collected by disconnecting the QA-2000 accelerometer from the SAMS electronics and connecting the input wires to each other to create an input voltage potential of 0 V. The difference obtained by averaging these data samples is then subtracted from each data sample.

[3]Axis misalignment correction involves correcting the data for each axis from the cross talk of acceleration whose source is from a direction perpendicular to the respective axis. This is accomplished by a fourth order equation, but its effects are small in comparison to bias and scale factor effects.

Y-axis values show that the standard deviation is 3.326 μg for the filtered data versus 3.079 μg for unfiltered data, thus a slightly better answer is obtained from the unfiltered data. When considering the effect of sensor hysteresis in the analysis, we get considerably better results of 0.092 μg for filtered data versus 0.172 μg for unfiltered data.[4]

The effects of using data that have been corrected for angular misalignment were also considered. This leads to some unique problems. Since bias is corrected before angular misalignment, we should have done the calculations on data that were not corrected for angular misalignment. This would have given us bias-free data to correct for angular misalignment. The problem with this is that the bias correction does not take measurement cross talk into account, unless the angular misalignment is taken into account. If the bias errors are calculated after correcting the data for angular misalignment, then the corrections must be applied after correcting the data for angular misalignment. This is not how we processed SAMS data, however.

Fortunately the data that were not corrected for angular misalignment provide slightly better results as shown in tables 15 to 18. Time 1N represents calculations performed on the data at time 1 which were uncorrected for angular misalignment. The designator F represents filtered data, while U represents unfiltered data.

CALIBRATION MODEL EFFECTS

As previously mentioned, it is desirable from a practical point of view to use the in-flight calibration data as a means to improve measurements taken in the controlled environment on Earth. Having examined the effects of each portion of the calibration processing on the data, we can now compare differences caused by the overall processing on the data in contrast to using the semiprocessed data itself.

To compare the absolute sensor bias of the semiprocessed measurement to the processed measurement, we need to first calculate the bias as predicted by the bias model at each of the respective temperatures for each axis and amplification level. This was done previously producing table 6. These calculated biases are labeled "predicted bias" in table 19. The sum of the calculated biases and the calibration model bias error measurement biases are labeled "corrected bias" in table 19, while the in-orbit measured biases are labeled "measured bias" in this table.

The Y-axis shows strong agreement between the measured bias and the bias obtained with the combination of ground measurement and in-flight correction. The errors that do exist are primarily associated with the source data being processed at different times causing different data sets to be selected for the calculations. This problem can be overcome by processing the different types of data at the same time. Additionally, using filtered data eases the task of selecting stable data segments for the calculations as illustrated by comparisons of figures 2, 4, and 6.

Additional information is available by comparing the differences between data processed by the new SAMS calibration temperature range data versus the old data. It was hoped that comparisons of this type would indicate how much better the new model predicts the bias than the old one did. The data shown in the three tables that follow were calculated based upon the same time intervals as those used in the previous tables.[5] One important difference in this data does exist, however. These old model calibration data were collected 8 months before STS–60 flew, while the new calibration data were collected only 2 weeks after STS–60 landed. The uncertainty caused by the bias drift over time may be corrected by repeating this procedure with a TSH that has calibrated with both models, or alternatively, repeating the calibration process for the new data after 7 months have passed.

Tables 20 to 23 show results of the same calculations in tables 7 to 10, except that the calculations were performed on data that have been processed with the old calibration model. Comparison of these data with the new model data show that the bias error of the new model are 6 to 20 μg smaller, while the values of absolute acceleration are comparable. The more typical value of 20 μg is within the margin of error introduced by the 8-month old data (ref. 1). It is worth mentioning that the old controlled X-axis G values are 0.1 μg closer to the ideal value of zero than are the new model readings. The cause of this unexpected improvement requires additional analysis.

[4]Consideration of sensor head hysteresis was primarily concerned with thermally induced effects. These effects were addressed by throwing away samples taken when the slope of temperature plot changed while the calibration procedure was being performed.

[5]The time interval used for the X-axis means at time 2 reverse, and time 3 forward, as well as the Y-axis time 3 reverse, were modified slightly to remove large asymmetrical disturbances seen in these data.

ACCURACY

The t-statistic model may be used as the basis of calculating the accuracy of the calculations performed. This can be used by determining the accuracy of the mean accelerations before and after the rotation process is calculated. The sum of the uncertainties then becomes the accuracy of our bias measurement.

Each of the two data sets used in the calculation must first be subdivided into n-subsets in order to provide a large enough sample size for the t-statistic. In our test we used ten sets of 6 sec each for our calculations. This gave interval widths for t_{95} of ± 0.2077 μg for the forward calculation and ± 0.1557 μg for the reverse calculation. The interval widths for t_{99} were ± 0.3148 μg for the forward calculation and ± 0.2239 μg for the reverse calculation. This yields accuracies of 0.3634 μg and 0.5387 μg with confidence intervals of 95 and 99 percent, respectively. These numbers confirm the basis for using the bias measurement on the control axis for the accuracy. The accuracies calculated with the t-statistic will be worse than those calculated by the bias measurement because the t-statistic uses shorter time intervals limiting the natural filtering of the mean calculation.

CONCLUSIONS

In-flight calibration of micro-accelerometers provides the capability to measure quasi-steady-state accelerations with an accuracy of 250 μg. The data presented here indicate bias uncertainties approaching 40 μg can be removed from the gravity data with a minimal amount of extra crew time required during the flight and only a few hours of analysis required post flight.

The procedure presented in this report will be repeated on future flights to obtain a larger sample size to better characterize the results. In addition, it will be repeated several times during the flight to characterize drift and repeatability. Additional tests on all three triaxial sensor heads are desired to test whether two sensors can be used to calibrate a third one by using the two sensors to determine the environment at the third one.

REFERENCE

1. Thomas, J.E.; Peters, R.B.; and Finley, B.D.: Space Acceleration Measurement System Triaxial Sensor Head Error Budget. NASA TM-105300, Jan. 1992.

TABLE 1.—AVERAGE TEMPERATURES FOR IDEAL SCALE FACTOR COMPUTATION (°C)

	Time 1 reverse	Time 1 forward	Time 2 forward	Time 2 reverse	Time 3 reverse	Time 3 forward
X-axis	16.65	16.66	17.81	17.79	17.66	17.62
Y-axis	18.15	17.98	18.18	18.06	17.89	17.86
Z-axis	17.95	17.82	17.96	17.90	17.75	17.72

TABLE 2.—AVERAGE IDEAL SCALE FACTORS (V/g)

	Time 1 reverse	Time 1 forward	Time 2 forward	Time 2 reverse	Time 3 reverse	Time 3 forward
X-axis	938.264	938.264	938.379	938.377	938.364	938.360
Y-axis	969.555	970.509	999.504	1000.260	1001.360	1001.550
Z-axis	−1272.300	−1273.520	−1272.150	−1272.800	−1274.530	−1274.240

TABLE 3.—MEAN ACCELERATIONS ON SEMIPROCESSED DATA (μg)

	Time 1 reverse	Time 1 forward	Time 2 forward	Time 2 reverse	Time 3 reverse	Time 3 forward
X-axis	−1269.34	−1271.61	−1264.74	−1264.98	−1263.83	−1263.65
Y-axis	981.48	981.60	973.77	984.33	984.42	975.66
Z-axis	−1260.04	−1258.73	−1249.69	−1258.82	−1260.10	−1252.94

TABLE 4.—AMBIENT GRAVITY ON SEMIPROCESSED DATA (μg)

	Time 1	Time 2	Time 3
Y-axis	0.057	−5.282	−4.379
Z-axis	0.657	4.568	3.580

TABLE 5.—BIAS AND AMBIENT GRAVITY MEASUREMENT ERROR ON SEMIPROCESSED DATA (μg)

	Time 1	Time 2	Time 3
X-axis	−1.136	0.116	0.090

TABLE 6.—BIAS ERRORS ON SEMIPROCESSED DATA (μg)

	Time 1	Time 2	Time 3
Y-axis	981.541	979.049	980.039
Z-axis	−1259.382	−1254.253	−1256.515

TABLE 7.—MEAN ACCELERATIONS ON UNFILTERED DATA (μg)

	Time 1 reverse	Time 1 forward	Time 2 forward	Time 2 reverse	Time 3 reverse	Time 3 forward
X-axis	−11.052	−9.834	−3.832	−4.491	−3.295	−2.963
Y-axis	−22.176	−21.155	−11.324	−18.805	−21.498	−16.309
Z-axis	36.788	38.898	38.323	31.087	30.792	39.289

TABLE 8.—AMBIENT GRAVITY ON UNFILTERED DATA (μg)

	Time 1	Time 2	Time 3
Y-axis	0.167	−4.892	−4.719
Z-axis	0.797	3.618	4.249

TABLE 9.—BIAS AND AMBIENT GRAVITY MEASUREMENT ERROR ON UNFILTERED DATA (μg)

	Time 1	Time 2	Time 3
X-axis	−0.345	0.331	0.166

TABLE 10.—CALCULATED MODEL BIAS ERRORS ON UNFILTERED DATA (μg)

	Time 1	Time 2	Time 3
Y-axis	21.837	16.215	16.459
Z-axis	38.056	34.705	35.040

TABLE 11.—MEAN ACCELERATIONS ON FILTERED DATA (μg)

	Time 1 reverse	Time 1 forward	Time 2 forward	Time 2 reverse	Time 3 reverse	Time 3 forward
X-axis	−9.899	−10.343	−4.172	−4.670	−4.104	−3.030
Y-axis	−22.691	−23.339	−11.862	−22.740	−22.526	−12.340
Z-axis	39.510	41.103	41.172	33.030	32.581	41.433

TABLE 12.—AMBIENT GRAVITY ON FILTERED DATA (μg)

	Time 1	Time 2	Time 3
Y-axis	−0.324	5.439	5.096
Z-axis	0.865	4.071	4.426

TABLE 13.—BIAS AND AMBIENT GRAVITY MEASUREMENT ERROR ON FILTERED DATA (μg)

	Time 1	Time 2	Time 3
X-axis	–0.222	0.249	0.252

TABLE 14.—CALCULATED MODEL BIAS ERRORS ON FILTERED DATA (μg)

	Time 1	Time 2	Time 3
Y-axis	–23.015	–17.301	–17.430
Z-axis	40.307	37.101	37.007

TABLE 15.—ANGULAR ALIGNMENT EFFECTS ON MEAN ACCELERATIONS (μg)

		Time 1 reverse	Time 1 forward	Time 1N reverse	Time 1N forward
X-axis	F	–11.641	–10.413	–11.584	–10.449
	U	–11.052	–9.834	–10.097	–9.869
Y-axis	F	–23.450	–22.801	–23.717	–25.302
	U	–22.176	–21.155	–22.177	–23.451
Z-axis	F	38.839	40.807	38.821	40.791
	U	36.788	38.898	36.771	38.883

TABLE 16.—ANGULAR ALIGNMENT EFFECTS ON AMBIENT GRAVITY (μg)

		Time 1	Time 1N
Y-axis	F	0.324	0.926
	U	0.511	–0.770
Z-axis	F	0.984	–0.985
	U	1.055	–1.056

TABLE 17.—ANGULAR ALIGNMENT EFFECTS ON BIAS AND AMBIENT GRAVITY MEASUREMENT ERRORS (μg)

		Time 1	Time 1N
X-axis	F	0.614	–0.567
	U	0.609	0.549

TABLE 18.—ANGULAR ALIGNMENT EFFECTS ON CALCULATED MODEL BIAS ERRORS (μg)

		Time 1	Time 1N
Y-axis	F	–23.126	–23.126
	U	–21.666	–21.666
Z-axis	F	39.823	39.806
	U	37.843	37.827

TABLE 19.—EFFECTS OF PROCESSING ON ABSOLUTE BIAS MEASUREMENTS

	Time 2 predicted bias, μg	Time 3 predicted bias, μg	Time 2 corrected bias, μg	Time 3 corrected bias, μg	Time 2 measured bias, μg	Time 3 measured bias, μg
Y-axis	−999.882	−1001.455	−982.581	−984.025	−979.049	−980.039
Z-axis	−1272.475	−1274.385	−1235.374	−1237.378	−1254.253	−1256.515

TABLE 20.—CALIBRATION EFFECTS ON MEAN ACCELERATIONS (μg)

		Time 1 reverse	Time 1 forward	Time 2 forward	Time 2 reverse	Time 2 reverse	Time 2 forward
X-axis	F	2.090	3.203	9.603	9.267	10.246	10.444
	U	1.959	3.037	9.192	8.734	9.681	10.040
Y-axis	F	50.703	51.164	42.054	31.652	31.981	40.408
	U	47.925	48.760	39.642	30.294	30.044	42.823
Z-axis	F	5.284	7.227	48.005	39.615	38.857	47.546
	U	5.067	7.154	44.786	37.314	36.721	45.067

TABLE 21.—CALIBRATION EFFECTS ON BIAS ERRORS (μg)

		Time 1	Time 2	Time 3
X-axis	F	2.647	9.435	10.345
	U	2.498	8.963	9.861
Y-axis	F	50.934	36.853	37.402
	U	48.342	34.968	35.422
Z-axis	F	6.256	43.810	43.202
	U	6.111	41.050	40.894

TABLE 22.—CALIBRATION EFFECTS ON AMBIENT GRAVITY (μg)

		Time 1	Time 2	Time 3
X-axis	F	0.556	0.168	0.099
	U	−0.539	0.229	0.179
Y-axis	F	0.231	5.201	5.421
	U	0.418	4.674	4.986
Z-axis	F	0.972	4.195	4.344
	U	1.044	3.736	4.173

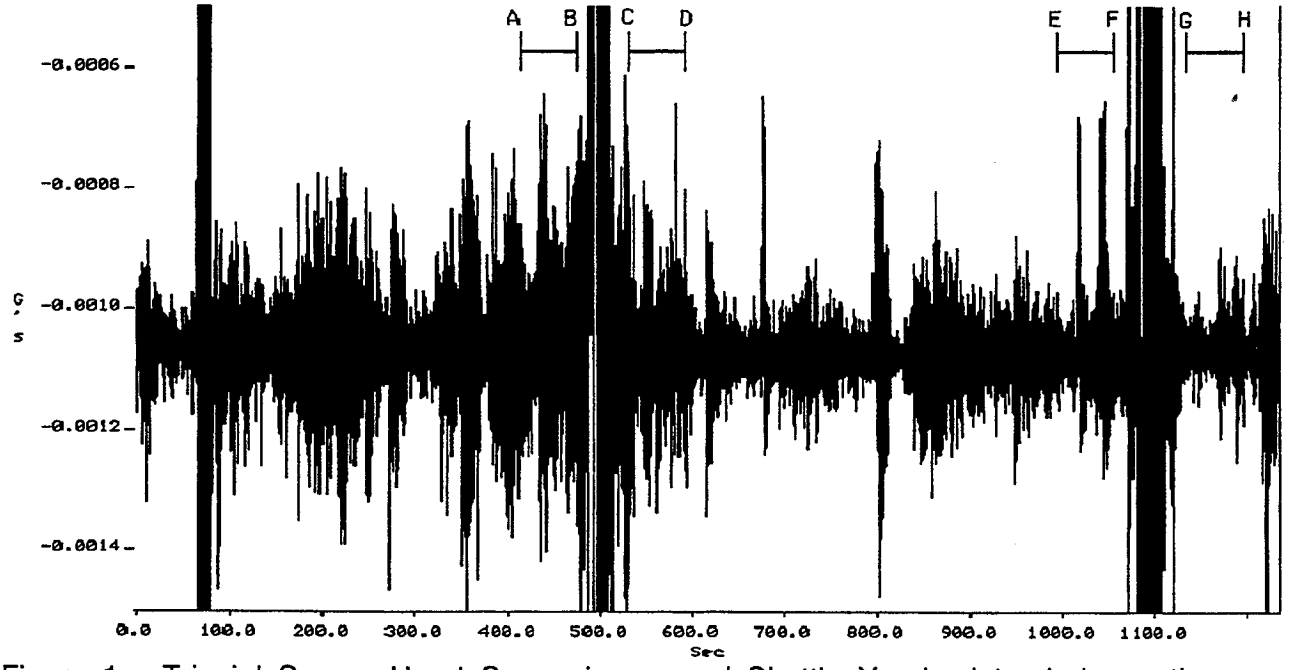

Figure 1 .–Triaxial Sensor Head C: semiprocessed Shuttle Y-axis data during entire calibration procedure.

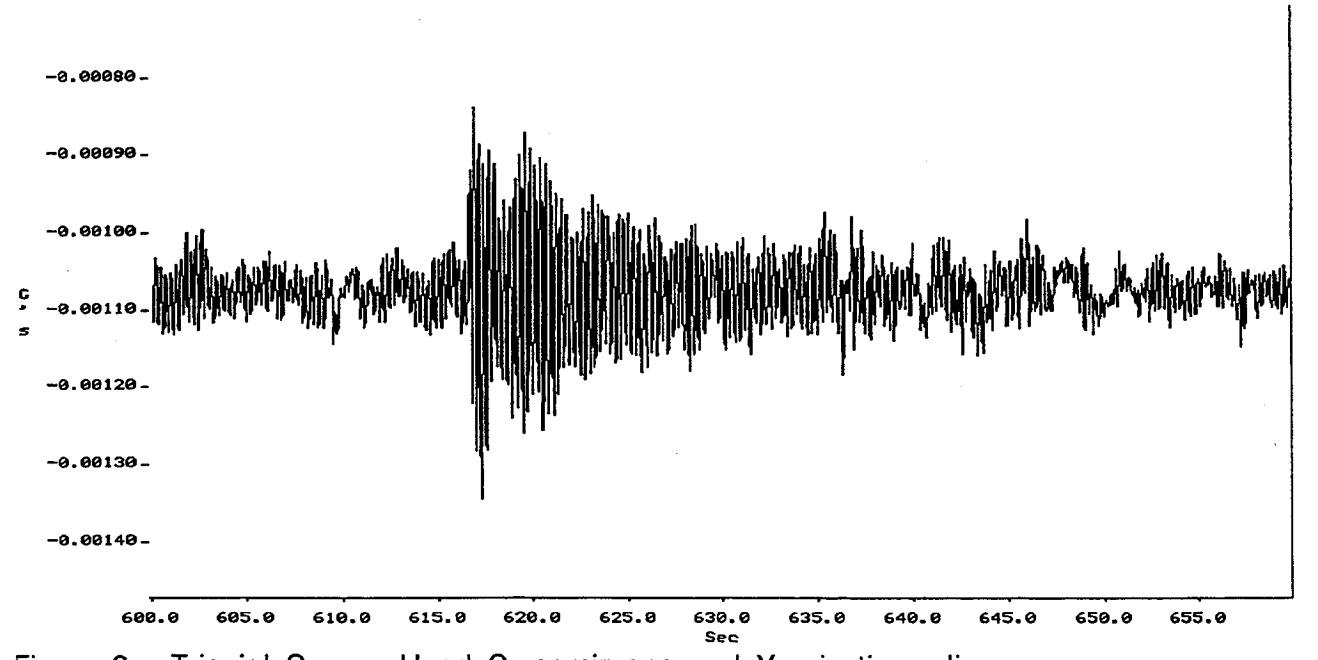

Figure 2 .–Triaxial Sensor Head C: semiprocessed Y-axis time slice.

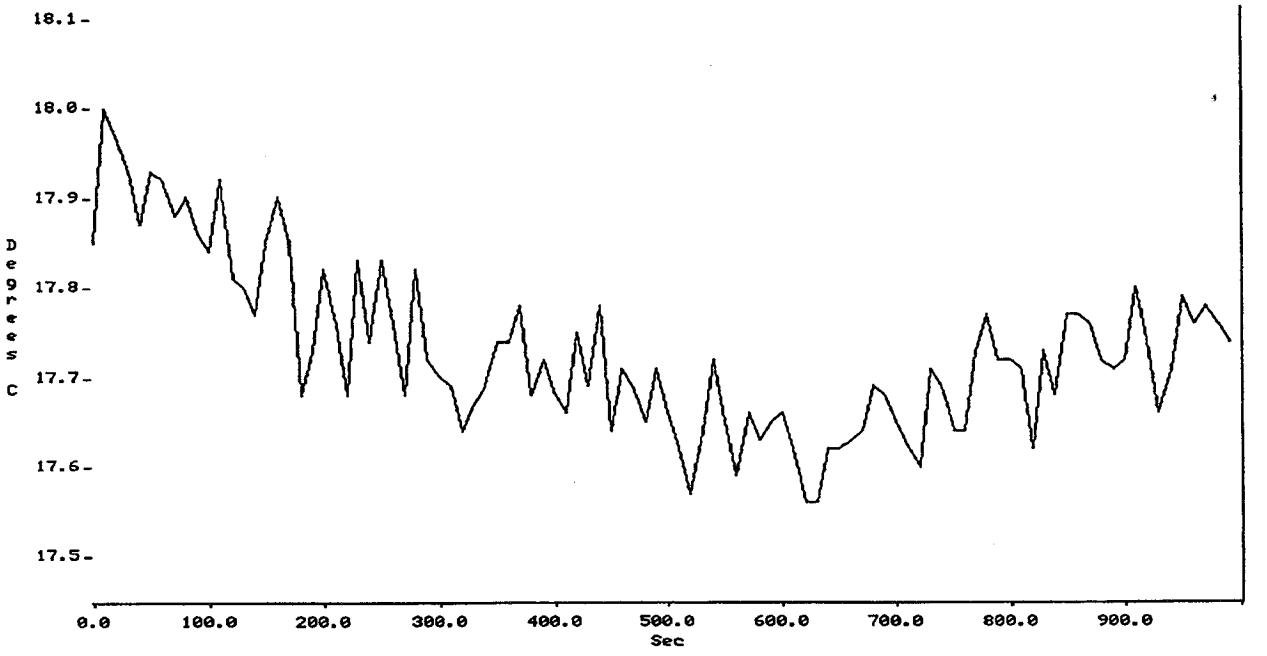

Figure 3 .–Change in slope of Y-axis temperature changes.

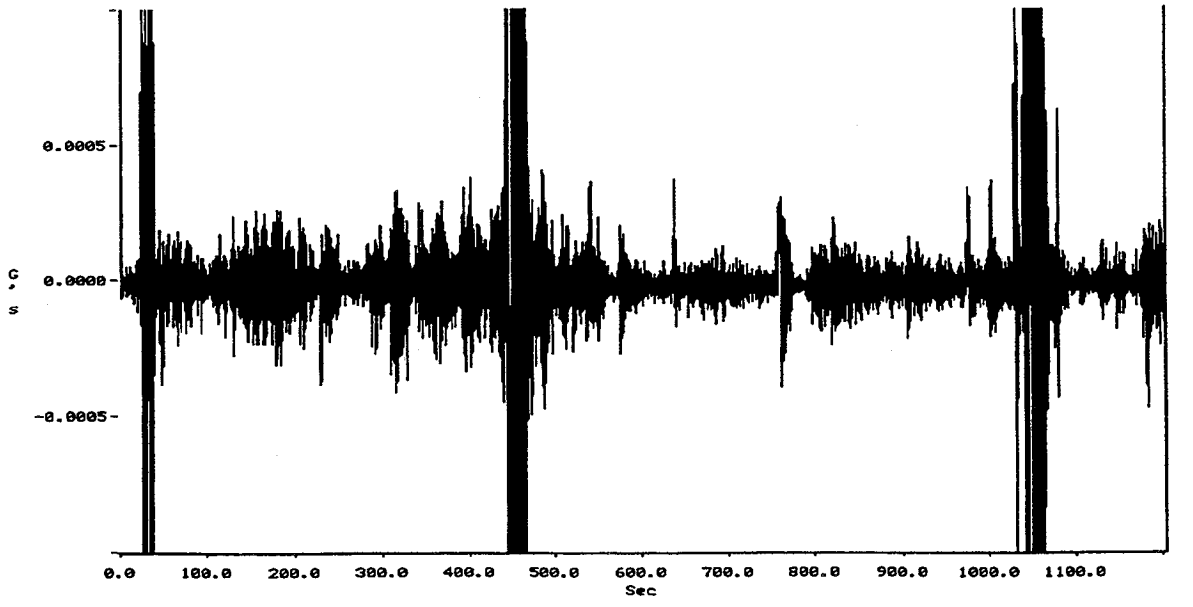

Figure 4 .–Triaxial Sensor Head C: processed Shuttle Y-axis.

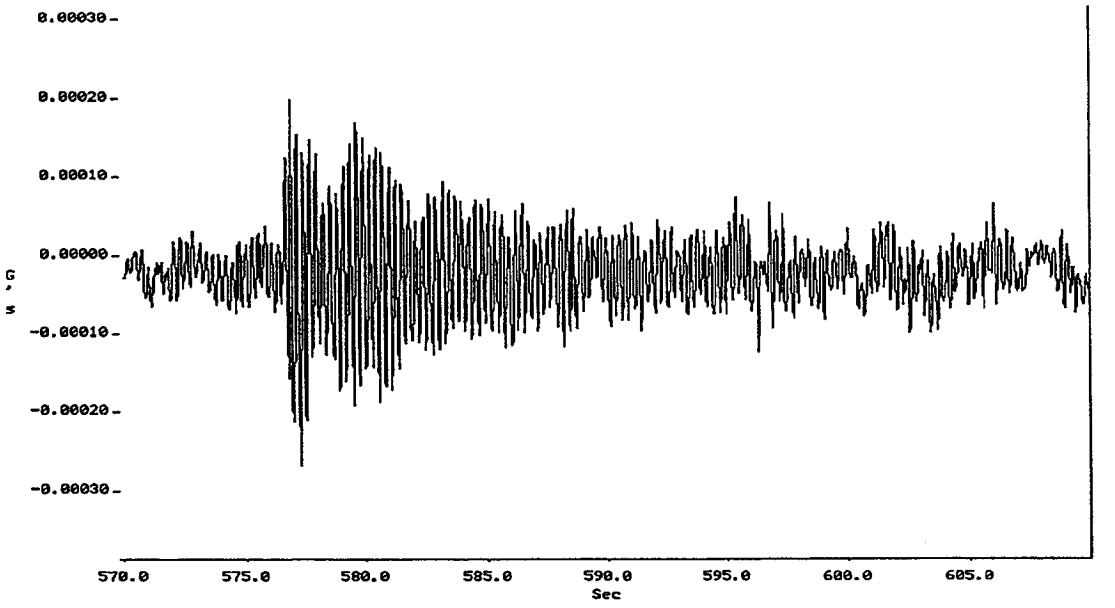

Figure 5 . –Triaxial Sensor Head C: processed Shuttle Y-axis time slice.

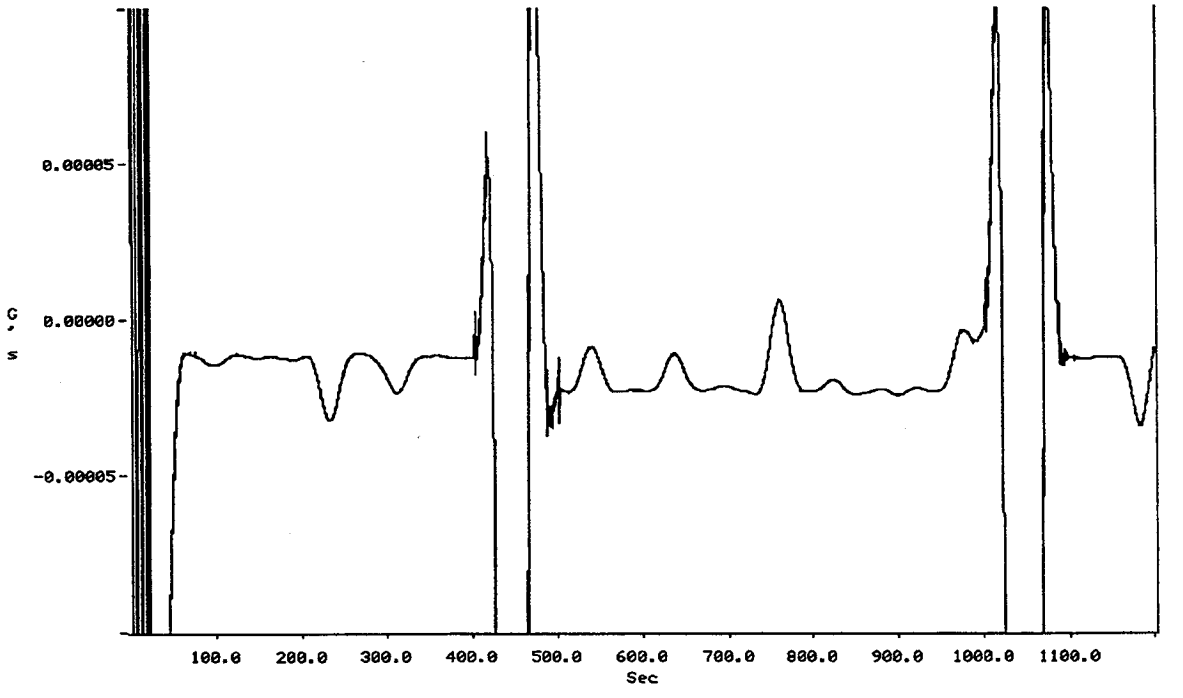

Figure 6 .–Triaxial Sensor Head C: filtered Y-axis.

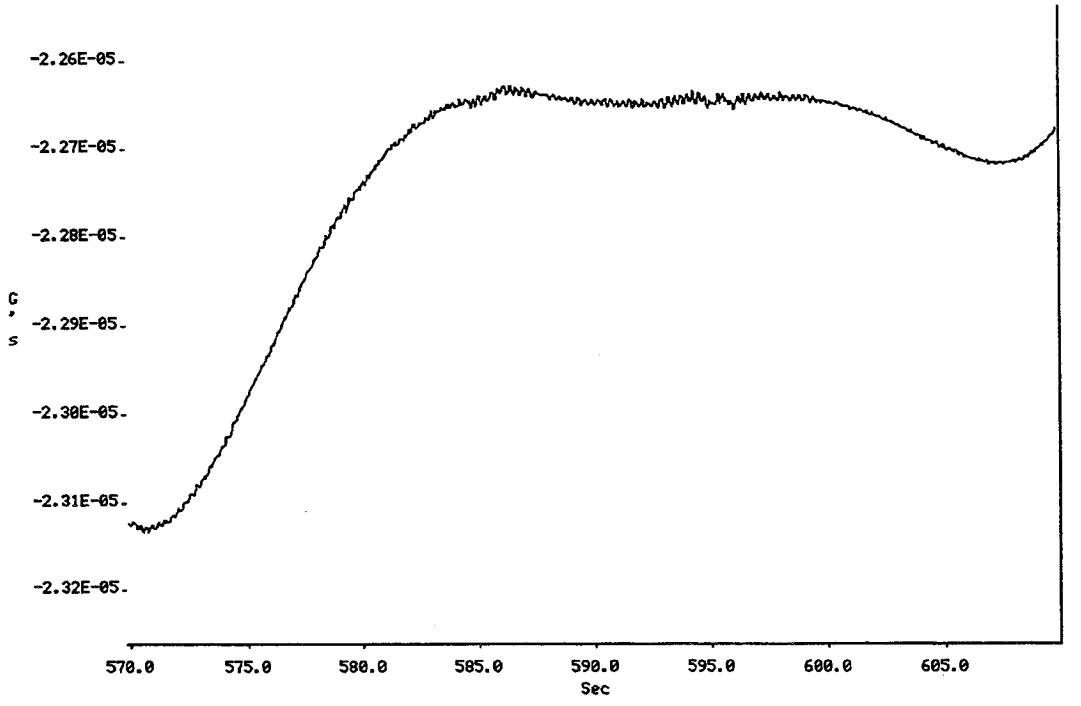

Figure 7 .–Filtered time slice.

REPORT DOCUMENTATION PAGE

Form Approved
OMB No. 0704-0188

1. AGENCY USE ONLY (*Leave blank*)	2. REPORT DATE	3. REPORT TYPE AND DATES COVERED
	June 1996	Technical Memorandum

4. TITLE AND SUBTITLE

In-Orbit Calibration of a SAMS Triaxial Sensor Head

5. FUNDING NUMBERS

WU–949–63–60

6. AUTHOR(S)

Louis S. Chestney and Ronald J. Sicker

7. PERFORMING ORGANIZATION NAME(S) AND ADDRESS(ES)

National Aeronautics and Space Administration
Lewis Research Center
Cleveland, Ohio 44135–3191

8. PERFORMING ORGANIZATION REPORT NUMBER

E–9746

9. SPONSORING/MONITORING AGENCY NAME(S) AND ADDRESS(ES)

National Aeronautics and Space Administration
Washington, D.C. 20546–0001

10. SPONSORING/MONITORING AGENCY REPORT NUMBER

NASA TM–106980

11. SUPPLEMENTARY NOTES

Louis S. Chestney, Aerospace Design & Fabrication, Inc., 3003 Aerospace Parkway, Brook Park, Ohio 44142, subcontractor to NYMA, Inc. (work funded by NASA Contract NAS3–27186) and Ronald J. Sicker, NASA Lewis Research Center. Responsible person, Ronald J. Sicker, organization code 6743, (216) 433–6498.

12a. DISTRIBUTION/AVAILABILITY STATEMENT

Unclassified - Unlimited
Subject Categories 19 and 88

This publication is available from the NASA Center for Aerospace Information, (301) 621–0390.

12b. DISTRIBUTION CODE

13. ABSTRACT (*Maximum 200 words*)

This report describes the results of in orbit calibration data collected for a Space Acceleration Measurement System (SAMS) Triaxial Sensor Head (TSH) and the methods used to process the data for bias and gravity levels.

14. SUBJECT TERMS

Shuttle mission; Calibration; Bias; Acceleration; STS–60; Spacehab–02

15. NUMBER OF PAGES

16

16. PRICE CODE

A03

17. SECURITY CLASSIFICATION OF REPORT	18. SECURITY CLASSIFICATION OF THIS PAGE	19. SECURITY CLASSIFICATION OF ABSTRACT	20. LIMITATION OF ABSTRACT
Unclassified	Unclassified	Unclassified	

National Aeronautics and
Space Administration

Lewis Research Center
21000 Brookpark Rd.
Cleveland, OH 44135-3191